HHS Public Access

Author manuscript

Hepatology. Author manuscript; available in PMC 2019 December 05.

Published in final edited form as:

Hepatology. 2019 December ; 70(6): 1972–1985. doi:10.1002/hep.30765.

Hepatocyte Deletion of Triglyceride-Synthesis Enzyme Acyl CoA: Diacylglycerol Acyltransferase 2 Reduces Steatosis Without Increasing Inflammation or Fibrosis in Mice

Nina L. Gluchowski[1,2,3], **Katlyn R. Gabriel**[2,3,4], **Chandramohan Chitraju**[2,3], **Roderick T. Bronson**[5], **Niklas Mejhert**[2,3], **Sebastian Boland**[2,3], **Kun Wang**[2,3], **Zon Weng Lai**[2,3], **Robert V. Farese Jr.**[2,3,6,*], **Tobias C. Walther**[2,3,4,6,*]

[1]Division of Gastroenterology and Nutrition, Boston Children's Hospital, Boston, MA

[2]Department of Genetics and Complex Diseases, Harvard T.H. Chan School of Public Health, Boston, MA

[3]Department of Cell Biology, Harvard Medical School, Boston, MA

[4]Howard Hughes Medical Institute, Boston, MA

[5]Rodent Histopathology Core, Harvard Medical School, Boston, MA

[6]Broad Institute of Harvard and Massachusetts Institute of Technology, Cambridge, MA

Abstract

Nonalcoholic fatty liver disease (NAFLD) is characterized by excess lipid accumulation in hepatocytes and represents a huge public health problem owing to its propensity to progress to nonalcoholic steatohepatitis, fibrosis, and liver failure. The lipids stored in hepatic steatosis (HS) are primarily triglycerides (TGs) synthesized by two acyl-CoA:diacylglycerol acyltransferase (DGAT) enzymes. Either DGAT1 or DGAT2 catalyzes this reaction, and these enzymes have been suggested to differentially utilize exogenous or endogenously synthesized fatty acids, respectively. DGAT2 has been linked to storage of fatty acids from *de novo* lipogenesis, a process increased in NAFLD. However, whether DGAT2 is more responsible for lipid accumulation in NAFLD and progression to fibrosis is currently unknown. Also, it is unresolved whether DGAT2 can be safely inhibited as a therapy for NAFLD. Here, we induced NAFLD-like disease in mice by feeding a diet rich in fructose, saturated fat, and cholesterol and found that hepatocyte-specific *Dgat2* deficiency reduced expression of *de novo* lipogenesis genes and lowered liver TGs by ~70%. Importantly, the reduction in steatosis was not accompanied by increased inflammation or fibrosis, and insulin and glucose metabolism were unchanged. *Conclusion:* This study suggests that hepatic

ADDRESS CORRESPONDENCE AND REPRINT REQUESTS TO: Robert V. Farese, Jr., M.D., Department of Genetics and Complex Diseases, Harvard T.H. Chan School of Public Health, Building 1, Room 505, 655 Huntington Avenue, Boston, MA 02115, robert@hsph.harvard.edu, Tel.: +1-617-432-3076, Tobias C. Walther, Ph.D., Department of Genetics and Complex Diseases, Harvard T.H. Chan School of Public Health, Building 1, Room 505, 655 Huntington Avenue, Boston, MA 02115, twalther@hsph.harvard.edu, Tel.: +1-617-432-3076.

*These authors contributed equally.

Potential conflict of interest: Nothing to report.

Supporting Information

Additional Supporting Information may be found at onlinelibrary.wiley.com/doi/10.1002/hep.30765/suppinfo.

DGAT2 deficiency successfully reduces diet-induced HS and supports development of DGAT2 inhibitors as a therapeutic strategy for treating NAFLD and preventing downstream consequences.

Nonalcoholic fatty liver disease (NAFLD) represents a huge public health problem, affecting ~1 billion people worldwide.[1] NAFLD is the hepatic manifestation of metabolic syndrome (MetS) and includes simple steatosis and nonalcoholic steatohepatitis (NASH). Approximately 25% of people with hepatic steatosis (HS) will develop NASH.[1] NAFLD/NASH can lead to complications such as fibrosis, cirrhosis, liver failure, and hepatocellular carcinoma.[2] There are no U.S. Food and Drug Administration (FDA)-approved medications to treat NAFLD, although multiple potential therapies are in phase III clinical trials.[3] Evidence suggests that treating NAFLD may be beneficial for preventing NASH and other sequalae. For example, studies evaluating paired biopsies in patients with NAFLD showed that isolated steatosis can progress to NASH with fibrosis over a median time span of 3.0 to 6.6 years.[4,5] In addition, a report from a joint workshop with members of the American Association for the Study of Liver Diseases and the FDA notes that resolution of steatohepatitis (SH) almost never occurs without improvement in steatosis.[6] Therefore, one approach to treating NAFLD/NASH is to prevent triglycerides (TGs) and other neutral lipids from accumulating in the liver.

Two enzymes, acyl CoA:diacylglycerol acyltransferase (DGAT)1 and DGAT2, catalyze the final step of TG synthesis.[7] Yet, these enzymes share no sequence similarity, and DGAT1 is a constitutive endoplasmic reticulum (ER) enzyme, whereas DGAT2 localizes around lipid droplets in addition to the ER.[8] In liver, DGAT1 preferentially utilizes exogenous fatty acids for TG synthesis.[9] In contrast, DGAT2 may preferentially utilize fatty acids from *de novo* lipogenesis.[9–11] In this respect, we showed previously that hepatic DGAT1 deficiency protected against steatosis from a high-fat diet, but did not protect against steatosis induced by increased *de novo* lipogenesis.[9]

It is unclear whether blocking TG synthesis by DGAT2 would be beneficial for treating human NAFLD. This is an important question, given that highly potent and specific inhibitors are available for DGAT2.[12–15] To address this question, DGAT2 activity was previously lowered in adult mice by inhibiting enzymatic activity or gene expression. In one study, both diet-induced and genetically obese mice were treated with DGAT2 antisense oligonucleotides (ASOs), which reduced *Dgat2* expression in liver (and adipose tissue) and decreased hepatic TG content.[16] Another study examined the effects of DGAT2 ASO treatment in obese and diabetic *db/db* mice fed a methionine-choline deficient (MCD) diet for 4–8 weeks.[17] This diet produces hepatic inflammation and fibrosis, but does not mimic other aspects of human MetS, such as weight gain and insulin resistance (IR).[18] DGAT2 ASO-treated mice had lower TG content after 4 weeks, but this difference was not found in mice on the diet for 8 weeks. The hepatic inflammation and fibrosis observed in MCD-diet-fed mice were exacerbated in DGAT2 ASO-treated animals, provoking concern for DGAT2 inhibition as a therapy.[17] However, ASO treatments themselves may be associated with toxicity.[19] Because of the uncertainty of DGAT2 deficiency in NAFLD and because *de novo* lipogenesis appears to be an important contributor to NAFLD in humans, contributing

to as much as 26% of liver TG fatty acids,[20] inhibition of DGAT2 warrants further investigation.

In the current study, we investigated the function of DGAT2 in progression of NAFLD/NASH in a murine model of human MetS. Given that global DGAT2 deficiency in mice results in death shortly after birth because of lipopenia and skin barrier defects,[21] we generated hepatocyte-specific *Dgat2* knockout (Liv*Dgat2*KO) mice. We fed these mice a diet rich in fructose, palmitate, and cholesterol (FPC), which produces HS, inflammation, and fibrosis in mice.[22] FPC-fed mice also have liver fatty acid changes similar to those reported in human NASH.[22] Our results provide insights into the role of DGAT2 deficiency in HS and provide information relevant to development of DGAT2 inhibitors as treatments for this disorder.

Materials and Methods

ANIMAL STUDIES

Mouse experiments were per Harvard Center for Comparative Medicine guidelines. Mice were maintained in a barrier facility (12-hour light/12-hour dark cycle) with *ad libitum* food and water, unless stated. Littermate controls were used. Mice were fed chow (PicoLab Rodent Diet 20 5053; LabDiet, St. Louis, MO) or FPC (TD.160785; Envigo, Madison, WI) diets.[22]

For glucose and insulin tolerance tests, mice were fasted for 16 hours or 4 hours, respectively. Glucose (2 g/kg body weight) or human insulin (1 unit/kg body weight; Lilly, Indianapolis, IN) was administered intraperitoneally. For TG secretion assays, mice were fasted for 4 hours. Tyloxapol (500 mg/kg; Sigma-Aldrich, St. Louis, MO) was administered intravenously. Plasma TG was measured using the Infinity Triglycerides Liquid Stable Reagent (Thermo Fisher Scientific, Waltham, MA).

IMMUNOBLOTTING

Tissues were lysed in buffer containing sucrose (250 mM), Tris Cl (50 mM; pH 7.4), and Complete Mini ethylenediaminetetraacetic acid (EDTA)-free protease inhibitor cocktail (Sigma-Aldrich) using a Dounce homogenizer. Samples (tissues or 1 μL of plasma) were denatured in Laemmli buffer, separated on a 4%−15% sodium dodecyl sulfate/polyacrylamide gel electrophoresis gel (BioRad, Hercules, CA), and transferred to a polyvinylidene difluoride membrane (BioRad). The membrane was blocked with Trisbuffered saline with Tween (TBST) containing 5% milk for 1 hour at room temperature and incubated with primary antibodies (4°C overnight for tissues, room temperature for 1 hour for plasma). The membrane was washed with TBST for 5 minutes three times, incubated with a secondary antibody at room temperature for 1 hour, washed again, and revealed using a SuperSignal West Pico chemiluminescent substrate kit (Thermo Fisher Scientific).

ANTIBODIES

Rabbit polyclonal antibodies against mouse DGAT1 and DGAT2 were generated (GenScript, Piscataway, NJ), affinity purified, and used at a 1:1,000 dilution.[23] Goat polyclonal antibody against apolipoprotein A1 (apo-A1; ab7614; Abcam, Cambridge, MA) was used at a 1:1,000 dilution.

qRT-PCR—Tissues were lysed in QIAzol (Qiagen, Germantown, MD) using a Bead Mill Homogenizer (VWR), and RNA was isolated using the RNeasy kit (QIAGEN, Hilden, Germany) per manufacturers' instructions. Complementary DNA (cDNA) was synthesized using an iScript cDNA synthesis kit (BioRad), and qRT-PCR was performed with a SYBR Green PCR Master Mix kit (Applied Biosystems, Thermo Fisher Scientific).

DGAT1 ACTIVITY ASSAYS

DGAT1 activity was measured *in vitro* under conditions selective for DGAT1.[23] Liver lysates (10 μg) were incubated with DGAT1 inhibitor,[24] where indicated.

PLASMA ANALYSIS

Plasma lipid and transaminases were measured using the Piccolo Lipid Panel Plus and Piccolo Liver Panel Plus used with a Piccolo Xpress chemistry analyzer (Abaxis). Ketones were measured using Wako Autokit Total Ketone Bodies per the manufacturer's instructions (FUJIFILM Wako Diagnostics, Mountain View, CA).

HISTOPATHOLOGICAL ANALYSIS

Liver samples were fixed in 4% formaldehyde overnight at 4°C. Sectioning and staining were performed at the Dana Farber/Harvard Cancer Center Rodent Histopathology Core. Paraffin-embedded samples were used for hematoxylin and eosin (H&E), Picro Sirius Red, and Masson's trichrome staining. Frozen sections were used for Oil Red O (ORO) staining. H&E-stained sections were used to assign steatosis and inflammation severity scores, and Picro Sirius Red–stained sections were used to assign fibrosis severity scores by three investigators, including an expert rodent histopathologist (R.T.B.).

MEASUREMENT AND ANALYSIS OF LIVER LIPIDS

Liver (~50 mg) was homogenized in 500 μL of lysis buffer (250 mM of sucrose, 50 mM of Tris Cl; pH 7.4) and cOmplete Mini EDTA-free protease inhibitor cocktail (Sigma-Aldrich). Lipids were extracted using the Bligh and Danner method, resuspended in 0.1%Triton X100, and sonicated five times at 30 mA for 1 second. TG and cholesterol were measured using Infinity Triglycerides Liquid Stable Reagent and Infinity Cholesterol Liquid Stable Reagent kits (Thermo Fisher Scientific).

LIPIDOMICS

Liver (~100 mg) was lysed in 1 mL of phosphate-buffered saline with a bead mill homogenizer (VWR, Radnor, PA). Lipids were extracted using Folch's method.[25] The organic phase of each sample, normalized by tissue weight, was separated using ultra-high-performance liquid chromatography coupled to tandem mass spectrometry.[26] See

Supporting Methods for details. All data were analyzed using the LipidSearch version 4.1 SP (Thermo Fisher Scientific), and all identified species (grade A, B, and C quality) were validated using R studio (RStudio Team [2015]; RStudio: Integrated Development for R; RStudio, Inc., Boston, MA; www.rstudio.com). The data were manually curated after computational analysis. Data are displayed as median fold change compared to control chow-fed animals, scaled linearly.

PROTEOMICS

For sample preparation and experimental details, please see the Supporting Methods section. Mass spectrometry data were analyzed by MaxQuant software version 1.5.2.8,[27] using the following setting: oxidized methionine residues and protein N-terminal acetylation as variable modification, cysteine carbamidomethylation as fixed modification, first search peptide tolerance 20 ppm, and main search peptide tolerance 4.5 ppm. Protease specificity was set to trypsin with up to two missed cleavages allowed. Only peptides longer than six amino acids were analyzed, and the minimal ratio count to quantify a protein is 2. The false discovery rate was set to 5% for peptide and protein identifications. Database searches were performed using the Andromeda search engine integrated into the MaxQuant environment[28] against the UniProt-mouse database containing 54,185 entries (December 2018). “Matching between runs” algorithm with a time window of 0.7 min was utilized to transfer identifications between samples processed using the same nanospray conditions. Protein tables were filtered to eliminate identifications from the reverse database and common contaminants. Data are available through ProteomeXchange with identifier PXD013423. To identify proteins regulated by diet/genotype, the data set was imported to R Studio and evaluated using a 2 × 2 factorial design in Linear Models for Microarray Data.[29] Pathway analyses for genes regulated by a fold change ≥ 2 and q values <0.05 were preformed using ToppFun[30] with gene limits 10–1000, calculation: disease.

STATISTICAL ANALYSIS

Data are presented as mean ± SD, unless otherwise stated. Statistical significance was evaluated with Student t test, two-way analysis of variance (ANOVA) with post-hoc Tukey test, or repeated-measures ANOVA for time-course experiments. Statistical analyses were done using Graphpad Prism 7 for Mac OS X Version 7.0d (Graphpad Software Inc., La Jolla, CA; www.graphpad.com).

Results

GENERATION AND VALIDATION OF LIV*DGAT2* KNOCKOUT MICE, A MURINE GENETIC MODEL OF DGAT2 DEFICIENCY IN HEPATOCYTES

To investigate the function of DGAT2 in liver, we generated Liv*Dgat2*KO mice by crossing *Dgat2*$^{flox/flox}$ mice of C57BL/6J background[23] with mice expressing Cre recombinase under control of the albumin promotor (B6.Cg-Tg(Alb-Cre)21MGN/J; The Jackson Laboratory, Bar Harbor, ME).[31] This caused deletion of exons 3–4 in *Dgat2* (Fig. 1A) and more than 80% reduction in *Dgat2* transcript levels in liver (Fig. 1B). The residual *Dgat2* mRNA detected likely originates in other cell types besides hepatocytes in liver. Despite some *Dgat2* mRNA expression, there was no detectable DGAT2 protein in liver

homogenates of Liv*Dgat2*KO mice (Fig. 1C). The knockout was specific to the liver given that *Dgat2* transcript and protein levels were unchanged in adipose tissue (Fig. 1B,C). Investigating whether DGAT1 activity increased in hepatocytes to compensate for loss of DGAT2, we found no changes in *Dgat1* mRNA expression (Fig. 1B), DGAT1 protein levels or activity in Liv*Dgat2*KO livers (Supporting Fig. S1A,B).

METABOLIC PARAMETERS IN CONTROL AND LIV*DGAT2*KO MICE ON CHOW AND FPC DIETS

To study the contribution of DGAT2 to progression of NAFLD and, in particular, the contribution to development of inflammation and fibrosis, we utilized the FPC diet, which has been shown to produce these outcomes.[22] The FPC diet contains 52.4% kcal from fat (46% saturated fatty acids, 26% trans-fats) and is rich in cholesterol (1.25% by weight, compared with chow diet containing 0.01%). The diet has increased sucrose content, and the water administered contained 42 g/L of 45% fructose/55% glucose.[22] This diet induces higher liver/body weight ratios and increases fasting blood glucose, plasma insulin, and circulating alanine aminotransferase (ALT).[22] For our studies, male and female mice were weaned to a chow diet. At 8 weeks of age, the mice either continued on a chow diet or were fed the FPC diet (Fig. 1D). One cohort was fed the FPC diet for 16 weeks before evaluation of liver disease endpoints. A second cohort was fed the FPC diet for 15 weeks before undergoing glucose and insulin tolerance tests and evaluation of hepatic TG secretion. Mice recovered for 1 week between each of these experiments, and liver endpoints were evaluated 2 weeks later (Fig. 1D). Starting age and duration for the FPC diet were based on what was reported to induce hepatic inflammation and fibrosis in mice.[22]

Liv*Dgat2*KO and control mice had similar body weights on chow and FPC diets, and Liv*Dgat2*KO mice had lower liver/body weight ratios on the FPC diet (Fig. 2A). FPC-fed mice did not gain as much weight as with other high-fat diets. The male mice in our study had an average body weight of ~30 g, which was similar to chow-fed mice. The average weight previously reported after 16 weeks on the FPC diet was ~35 g.[22] The reason for the lower weight gain is unclear, but could be related to the diet being intrinsically more toxic. Liv*Dgat2*KO mice and controls had similar random blood glucose levels on chow diet (not shown) and similar glucose and insulin tolerance on FPC diet (Fig. 2B). Circulating levels of TG were lower in Liv*Dgat2*KO female mice on chow diet. However, this was not observed in males or in either sex on the FPC diet (Fig. 2C). Previous studies showed that the rate of hepatic TG secretion is reduced in lean mice treated with a DGAT2 inhibitor[14] and in diet-induced obese mice treated with DGAT2-ASO.[16] In our study, Liv*Dgat2*KO mice on the FPC diet showed reduced hepatic TG secretion, as measured after treatment with Tyloxapol, a lipoprotein lipase inhibitor (Fig. 2D).

Total cholesterol and high-density lipoprotein (HDL) cholesterol (HDL-C) levels were lower in both male and female Liv*Dgat2*KO mice on both diets (Fig. 2C). HDL-C levels were decreased by 26%−54%. The differences on chow diet did not reach statistical significance, possibly because of smaller numbers of mice in these groups. To investigate possible explanations for the reduced HDL-C phenotype, we examined expression of apolipoprotein

genes and found a decrease in apo-A1 transcript levels in Liv*Dgat2*KO FPC-fed mice (Fig. 2E). Apo-A1 protein levels were also decreased in plasma of Liv*Dgat2*KO mice (Fig. 2F).

LIV*DGAT2*KO MICE FED THE FPC DIET HAVE REDUCED STEATOSIS

To evaluate FPC-fed mice for steatosis, we stained liver sections with H&E and ORO. Images of liver sections of chow-fed mice are provided in Supporting Fig. S2A. Steatosis scores (0–4; Supporting Fig. S2B) were lower for Liv*Dgat2*KO mice than controls (Fig. 3A). Notably, macrosteatosis in livers of FPC-fed mice was predominantly in the periportal areas and found in both genotypes (Fig. 3A). Mice with severe steatosis, mainly control mice, had excess neutral lipids in both the periportal and centrilobular zones. Steatosis in centrilobular areas was generally microsteatosis and was reduced with DGAT2 deficiency (Fig. 3A).

Liv*Dgat2*KO mice had lower hepatic TG content, whereas hepatic total cholesterol content was similar between genotypes (Fig. 3B). Examination of gene expression in this cohort confirmed that *Dgat1* expression was similar between genotypes (Fig. 3C), even on the high-fat diet. Hepatic mRNA levels of lipogenic genes were higher in FPC-fed mice than those of the chow-fed cohort and lower in Liv*Dgat2*KO mice than in control mice on the FPC diet (Fig. 3D). Proteomic analysis revealed that several proteins which are targets of sterol regulatory element-binding protein were decreased in livers of chow- and FPC-fed Liv*Dgat2*KO mice compared to control mice (Fig. 3D), which is consistent with decreased lipogenesis. mRNA and protein levels of beta-oxidation genes were similar among genotypes (Fig. 3E). There was a modest increase in plasma ketones in male Liv*Dgat2*KO mice, possibly indicating increased fatty acid oxidation in the setting of decreased TG synthesis (Supporting Fig. S3).

To further investigate liver lipid composition of Liv*Dgat2*KO and control mice, we performed lipidomic analyses on livers from chow- and FPC-fed male mice. There were multiple changes between diets and genotypes (Fig. 4). Notably, diacylglycerol followed the same pattern as TG, and levels were increased on the FPC diet, although to a lesser extent in Liv*Dgat2*KO mice (Fig. 4A). Livers of Liv*Dgat2*KO mice incorporated a higher percentage of palmitate into these neutral lipids (Fig. 4A). This could be attributed to decreased desaturation of palmitate in Liv*Dgat2*KO mice secondary to down-regulation of stearoyl-Co-A desaturase 1 (*Scd1*; not shown), which is a target of sterol response element-binding protein 1c (SREBP1c). Hepatic *Scd1* expression was also decreased when inhibiting DGAT2 expression.[16] In our study, cholesterol esters were the lipid species that showed the largest relative increase on the FPC diet (Fig. 4B), presumably as a result of the excess cholesterol in the diet. Livers of Liv*Dgat2*KO mice stored even more cholesterol esters (Fig. 4B), likely as a way to esterify fatty acids that could not be stored in TG.

LIV*DGAT2*KO AND CONTROL MICE HAVE SIMILAR LEVELS OF INFLAMMATION AND FIBROSIS ON FPC DIET

A key question is whether inhibition of DGAT2 and reduced TG storage would result in increased inflammation or fibrosis. We examined H&E-stained liver sections of FPC-fed mice (Fig. 5A and Supporting Fig. S2B) and found similar levels of hepatic inflammation in both genotypes (Fig. 5B). In addition, there were no differences in circulating ALT levels

between genotypes, and, as expected, ALT values were increased in FPC-fed mice (Fig. 5B). mRNA levels of inflammatory response and ER stress genes were increased in FPC-fed mice and were similar between genotypes (Fig. 5C).

Liver sections were stained with Sirius Red and Masson's trichrome to evaluate collagen deposition (Fig. 5D and Supporting Fig. S2B). Images of liver sections of chow-fed mice are shown in Supporting Fig. S2A for reference. Fibrosis scores were similar in Liv*Dgat2*KO mice and controls (Fig. 5D). mRNA levels of genes associated with fibrosis and hepatic stellate cell activation were higher in mice on the FPC diet, but were similar between genotypes (Fig. 5E,F). Pathway analyses of proteomics data using TopFunn[30] revealed that the hepatic proteins increased by the FPC diet are associated with liver cirrhosis, liver injury, and SH (data not shown).

NASH outcomes were evaluated in a second cohort of FPC-fed mice over a longer period of time (19 weeks). Again, we observed improvement in steatosis (Supporting Fig. S5A). In this cohort, there were no differences in inflammation scores or gene expression, although a trend toward improvement in fibrosis was found in Liv*Dgat2*KO mice (Supporting Fig. S5A,B). These data suggest that DGAT2 deficiency in hepatocytes and the resulting lower TG content do not exacerbate inflammation and could be protective over longer periods of time.

Discussion

We show here that hepatocyte-specific *Dgat2* knockout results in decreased HS, with lower diacylglycerol and TG content, in mice fed the FPC diet, which induces fat accumulation and injury. Importantly, we found no worsening of liver inflammation or fibrosis with DGAT2 deficiency on this diet and a tendency toward improvement at longer times.

We found an ~70% reduction in hepatic TG content for FPC-fed Liv*Dgat2*KO mice. This study evaluated the function of hepatic DGAT2 in both male and female mice, which had 66%−71% reductions of TG, respectively. In general, FPC-fed mice developed macrosteatosis in the periportal areas and microsteatosis in the centrilobular areas. Hepatic DGAT2 deficiency appeared to prevent mostly the progression of microsteatosis. The degree of TG reduction we found was similar to that found in mice with adeno-associated virus/short hairpin RNA–mediated hepatic DGAT2 knockdown on a high-fat diet (60% kcal from fat).[14] A reduction of approximately 50%−60% liver TG was reported in mice and rats with inhibition of DGAT2 expression using ASOs[16,32] or a small-molecule inhibitor.[14] The marked and consistent improvement in steatosis in rodents with DGAT2 deficiency could be, in part, attriibuted to the high relative expression of *Dgat2* (versus *Dgat1*) in rodents[14] and the reduced ability of DGAT1 to utilize endogenously synthesized fatty acids as substrates.[9] The mice in our study were fed a diet high in fat, cholesterol, glucose, and fructose, therefore providing an excess of exogenous fatty acids, as well as abundant substrates for *de novo* lipogenesis. Consequently, FPC-fed mice increase *de novo* lipogenesis gene expression, and this effect is blunted in Liv*Dgat2*KO mice, which, in part, may explain the improvement in steatosis. Therefore, DGAT2 deficiency in the liver not only decreases TG synthesis, but also likely decreases *de novo* lipogenesis, which could explain why

diacylglycerols did not accumulate in Liv*Dgat2*KO livers (Fig. 4A). These findings are consistent with previous work that showed liver *Dgat2* overexpression increased lipogenic gene expression[33] and a study in which inhibition of DGAT2 expression decreased expression of genes involved in *de novo* lipogenesis.[16] The mechanism linking DGAT2 expression with regulation of *de novo* lipogenesis is yet unknown. In contrast to the reduction in hepatic TG content, cholesterol esters were increased in livers of Liv*Dgat2*KO FPC-fed mice fed. The FPC diet is rich in cholesterol, and given that fewer fatty acids are stored in TG with DGAT2 deficiency, these substrates may have driven cholesterol ester synthesis. Increased cholesterol ester synthesis could protect hepatocytes given that both unesterified fatty acids and free cholesterol in excess may be toxic.[34,35]

Hepatic DGAT2 deficiency improved steatosis, but did not worsen development of inflammation or fibrosis in mice on the FPC diet. This is in contrast to a study using DGAT2-ASO treatment in *db/db* mice fed an MCD diet.[17] However, the latter study utilized a nutrient-deficient diet to induce hepatic inflammation and fibrosis, which does not mimic other features of MetS, and, in fact, mice on the MCD diet lose weight.[18] Also, DGAT2 was inhibited by using ASO treatment, which may have off-target effects, such as decreasing DGAT2 expression in the adipose[16] or causing hepatotoxicity independent of the intended target.[19] In our study, the findings of similar degrees of inflammation and fibrosis between genotypes with different hepatic TG content suggests that the amount of hepatic TG is not solely responsible for disease progression. A limitation of interpreting the NASH endpoints in our study is that we found only modest development of fibrosis over several weeks. We can conclude that Liv*Dgat2*KO does not aggravate fibrosis in this setting, but we are unable to conclude whether this approach may prevent more severe fibrosis over longer study periods.

An important question is whether hepatic DGAT2 deficiency alters glucose metabolism. We note that FPC-fed Liv*Dgat2*KO mice exhibited no impairments in glucose and insulin tolerance, despite reductions in hepatic TG and diacylglycerol levels. This is consistent with other reports[14,16] and supports the concept that changes in hepatic diacylglycerol or TG do not always correlate with IR.[36] Our group previously reported that hepatic DGAT2 overexpression in mice does not change glucose or insulin tolerances, and these mice with increased liver TG had normal hyperinsulinemic-eyglycemic clamp studies.[33] However, our findings contrast with a study reporting IR in mice with overexpression of hepatic DGAT2[37] and another showing improved insulin sensitivity in high-fat-diet–fed rats treated with DGAT2 ASO.[32]

Surprisingly, we found a 26%−54% reduction in HDL-C levels in Liv*Dgat2*KO mice. This adds to the growing evidence that DGAT2 activity affects levels of circulating HDL-C. Similar decreases were found in mice treated with AAV-shDGAT2 or a DGAT2 inhibitor.[14] A low HDL-C level (~25 mg/dL) was also reported in a proband with nonsense mutation in *DGAT2*,[38] and an exome-wide association study showed that humans who are heterozygous for a nonsense mutation in *DGAT2* have lower HDL-C levels.[39] Our data show that a low HDL-C phenotype is reproduced in a murine model where DGAT2 is deficient only in hepatocytes. Although the mechanism of decreased circulating HDL-C remains unclear, our findings indicate that DGAT2 deficiency down-regulates hepatic

expression of apo-A1, likely resulting in decreased circulating levels of this protein. This suggests that there are fewer HDL particles per volume and not smaller HDL particles in circulation in Liv*Dgat2*KO mice. This may be of concern for therapeutic development of DGAT2 inhibitors in humans given that lower HDL-C is associated with cardiovascular disease.[40] However, the relationship of plasma HDL-C levels to coronary heart disease is complex,[41] making it uncertain how to interpret this finding. Also, it is unclear how hepatic DGAT2 deficiency may regulate apo-A1 gene expression.

Inhibition of DGAT2 is being considered as a therapy for NAFLD/NASH in humans.[12,14,15] In this respect, our findings in mice suggest that DGAT2 inhibition could be effective in lowering hepatic fat content in humans and may do so without increased risk of inflammation and injury. Additionally, we found no adverse effects on insulin sensitivity with DGAT2 deletion in liver. The reductions in HDL-C and apo-A1 levels we found with hepatic DGAT2 deficiency are of uncertain significance and require further investigation. However, our findings support the idea that further testing of DGAT2 inhibitors in the clinical setting is warranted.

Supplementary Material

Refer to Web version on PubMed Central for supplementary material.

Acknowledgment

We thank Jane Lee for assistance with animal experiments; the Dana-Farber/Harvard Cancer Center in Boston, Massachusetts for use of the Rodent Histopathology Core supported, in part, by an NCI Cancer Center Support Grant #NIH5P30 CA06516, which provided tissue processing, sectioning, and staining services; Merck & Co., Inc. for gift of DGAT1 inhibitor; Drs. Ira Tabas, Xiabo Wang, and Tina Herfel for discussions about the FPC diet; Drs. Morris Birnbaum, Kendra Bence, and Robert Dullea at Pfizer, Inc. for helpful discussions; and Gary Howard for editorial assistance.

Supported, in part, by National Institute of Diabetes and Digestive and Kidney Diseases Grants R01 DK101579 (to R.V.F.) and a North American Society of Pediatric Gastroenterology, Hepatology and Nutrition Young Investigator/Nestle Nutrition award (to N.L.G.). Tobias Walther is an investigator of the Howard Hughes Medical Institute. The content is solely the responsibility of the authors and does not necessarily represent the official views of the National Institutes of Health.

Abbreviations

ALT	alanine aminotransferase
apo-A1	apolipoprotein A1
ASOs	antisense oligonucleotides
DGAT	acyl CoA:diacylglycerol acyltransferase
ER	endoplasmic reticulum
FPC	fructose-palmitate-cholesterol
HDL	high-density lipoprotein
HDL-C	high-density lipoprotein cholesterol

H&E	hematoxylin and eosin
HS	hepatic steatosis
IR	insulin resistance
MCD	methionine-choline deficient
MetS	metabolic syndrome
NAFLD	nonalcoholic fatty liver disease
NASH	nonalcoholic steatohepatitis
ORO	Oil Red O
SREBP1c	sterol response element-binding protein 1c
TG	triglyceride

REFERENCES

1). Perumpail BJ, Khan MA, Yoo ER, Cholankeril G, Kim D, Ahmed A. Clinical epidemiology and disease burden of nonalcoholic fatty liver disease. World J Gastroenterol 2017;23: 8263–8276. [PubMed: 29307986]

2). Nasr P, Ignatova S, Kechagias S, Ekstedt M. Natural history of nonalcoholic fatty liver disease: a prospective follow-up study with serial biopsies. Hepatol Commun 2018;2:199–210. [PubMed: 29404527]

3). Alkhouri N, Scott A. An update on the pharmacological treatment of nonalcoholic fatty liver disease: beyond lifestyle modifications. Clin Liver Dis 2018;11:82–86.

4). McPherson S, Hardy T, Henderson E, Burt AD, Day CP, Anstee QM. Evidence of NAFLD progression from steatosis to fibrosingsteatohepatitis using paired biopsies: implications for prognosis and clinical management. J Hepatol 2015;62:1148–1155. [PubMed: 25477264]

5). Wong VW, Wong GL, Choi PC, Chan AW, Li MK, Chan HY, et al. Disease progression of non-alcoholic fatty liver disease: a prospective study with paired liver biopsies at 3 years. Gut 2010;59:969–974. [PubMed: 20581244]

6). Sanyal AJ, Friedman SL, McCullough AJ, Dimick-Santos L. Challenges and opportunities in drug and biomarker development for nonalcoholic steatohepatitis: findings and recommendations from an American Association for the Study of Liver Diseases-U.S. Food and Drug Administration Joint Workshop. Hepatology 2015;61:1392–1405. [PubMed: 25557690]

7). Harris CA, Haas JT, Streeper RS, Stone SJ, Kumari M, Yang K, et al. DGAT enzymes are required for triacylglycerol synthesis and lipid droplets in adipocytes. J Lipid Res 2011;52:657–667. [PubMed: 21317108]

8). Stone SJ, Levin MC, Zhou P, Han J, Walther TC, Farese RV. The endoplasmic reticulum enzyme DGAT2 is found in mitochondria-associated membranes and has a mitochondrial targeting signal that promotes its association with mitochondria. J Biol Chem 2009;284:5352–5361. [PubMed: 19049983]

9). Villanueva CJ, Monetti M, Shih M, Zhou P, Watkins SM, Bhanot S, et al. Specific role for acyl CoA: Diacylglycerol acyltransferase 1 (Dgat1) in hepatic steatosis due to exogenous fatty acids. Hepatology 2009;50:434–442. [PubMed: 19472314]

10). Qi J, Lang W, Geisler JG, Wang P, Petrounia I, Mai S, et al. The use of stable isotope-labeled glycerol and oleic acid to differentiate the hepatic functions of DGAT1 and −2. J Lipid Res 2012;53:1106–1116. [PubMed: 22493088]

11). Wurie HR, Buckett L, Zammit VA. Diacylglycerol acyltransferase 2 acts upstream of diacylglycerol acyltransferase 1 and utilizes nascent diglycerides and de novosynthesized fatty acids in HepG2 cells. FEBS J 2012;279:3033–3047. [PubMed: 22748069]

12). Kim MO, Lee S, Choi K, Lee S, Kim H, Kang H, et al. Discovery of a novel class of diacylglycerol acyltransferase 2 inhibitors with a 1H-pyrrolo[2,3-b]pyridine core. Biol Pharm Bull 2014;37:1655–1660. [PubMed: 25099343]

13). Imbriglio JE, Shen DM, Liang R, Marby K, You M, Youm HW, et al. Discovery and pharmacology of a novel class of diacylglycerol acyltransferase 2 inhibitors. J Med Chem 2015;58:9345–9353. [PubMed: 26561979]

14). McLaren DG, Han S, Murphy BA, Wilsie L, Stout SJ, Zhou H, et al. DGAT2 inhibition alters aspects of triglyceride metabolism in rodents but not in non-human primates. Cell Metab 2018;27:1236–1248.e6. [PubMed: 29706567]

15). Pabst B, Futatsugi K, Li Q, Ahn K. Mechanistic characterization of long residence time inhibitors of diacylglycerol acyltransferase 2 (DGAT2). Biochemistry 2018;57:6997–7010. [PubMed: 30422629]

16). Yu XX, Murray SF, Pandey SK, Booten SL, Bao D, Song XZ, et al. Antisense oligonucleotide reduction of DGAT2 expression improves hepatic steatosis and hyperlipidemia in obese mice. Hepatology 2005;42:362–371. [PubMed: 16001399]

17). Yamaguchi K, Yang L, McCall S, Huang J, Yu XX, Pandey SK, et al. Inhibiting triglyceride synthesis improves hepatic steatosis but exacerbates liver damage and fibrosis in obese mice with nonalcoholic steatohepatitis. Hepatology 2007;45:1366–1374. [PubMed: 17476695]

18). Machado MV, Michelotti GA, Xie G, de Almeida TP, Boursier J, Bohnic B, et al. Mouse models of diet-induced nonalcoholic steatohepatitis reproduce the heterogeneity of the human disease. PLoS One 2015;10:e0127991. [PubMed: 26017539]

19). Kamola PJ, Maratou K, Wilson PA, Rush K, Mullaney T, McKevitt T, et al. Strategies for in vivo screening and mitigation of hepatotoxicity associated with antisense drugs. Mol Ther Nucleic Acids 2017;8:383–394. [PubMed: 28918038]

20). Donnelly KL, Smith CI, Schwarzenberg SJ, Jessurun J, Boldt MD, Parks EJ. Sources of fatty acids stored in liver and secreted via lipoproteins in patients with nonalcoholic fatty liver disease. J Clin Invest 2005;115:1343–1351. [PubMed: 15864352]

21). Stone SJ, Myers HM, Watkins SM, Brown BE, Feingold KR, Elias PM, et al. Lipopenia and skin barrier abnormalities in DGAT2-deficient mice. J Biol Chem 2004;279:11767–11776. [PubMed: 14668353]

22). Wang X, Zheng Z, Caviglia JM, Corey KE, Herfel TM, Cai B, et al. Hepatocyte TAZ/WWTR1 promotes inflammation and fibrosis in nonalcoholic steatohepatitis. Cell Metab 2016;24: 848–862. [PubMed: 28068223]

23). Chitraju C, Walther TC, Farese RV Jr., The triglyceride synthesis enzymes DGAT1 and DGAT2 have distinct and overlapping functions in adipocytes. J Lipid Res 2019 4 1 pii: jlr.M093112. 10.1194/jlr.M093112. [Epub ahead of print].

24). Liu J, Gorski JN, Gold SJ, Chen D, Chen S, Forrest G, et al. Pharmacological inhibition of diacylglycerol acyltransferase 1 reduces body weight and modulates gut peptide release-Potential insight into mechanism of action. Obesity 2013;21:1406–1415. [PubMed: 23671037]

25). Folch J, Lees M, Sloane Stanley GH. A simple method for the isolation and purification of total lipides from animal tissues. J Biol Chem 1957;226:497–509. [PubMed: 13428781]

26). Narváez-Rivas M, Zhang Q. Comprehensive untargeted lipidomic analysis using core–shell C30 particle column and high field orbitrap mass spectrometer. J Chromatogr A 2016;1440:123–134. [PubMed: 26928874]

27). Cox J, Mann M. MaxQuant enables high peptide identification rates, individualized p.p.b.-range mass accuracies and proteome-wide protein quantification. Nat Biotechnol 2008;26:1367–1372. [PubMed: 19029910]

28). Cox J, Neuhauser N, Michalski A, Scheltema RA, Olsen JV, Mann M. Andromeda: a peptide search engine integrated into the MaxQuant environment. J Proteome Res 2011;10:1794–1805. [PubMed: 21254760]

29). Ritchie ME, Phipson B, Wu D, Hu Y, Law CW, Shi W, et al. limma powers differential expression analyses for RNA-sequencing and microarray studies. Nucleic Acids Res 2015;43:e47. [PubMed: 25605792]

30). Chen J, Bardes EE, Aronow BJ, Jegga AG. ToppGene Suite for gene list enrichment analysis and candidate gene prioritization. Nucleic Acids Res 2009;37:W305–W311. [PubMed: 19465376]

31). Postic C, Shiota M, Niswender KD, Jetton TL, Chen Y, Moates JM, et al. Dual roles for glucokinase in glucose homeostasis as determined by liver and pancreatic beta cell-specific gene knockouts using Cre recombinase. J Biol Chem 1999;274:305–315. [PubMed: 9867845]

32). Choi CS, Savage DB, Kulkarni A, Yu XX, Liu ZX, Morino K, et al. Suppression of diacylglycerol acyltransferase-2 (DGAT2), but not DGAT1, with antisense oligonucleotides reverses dietinduced hepatic steatosis and insulin resistance. J Biol Chem 2007;282:22678–22688. [PubMed: 17526931]

33). Monetti M, Levin MC, Watt MJ, Sajan MP, Marmor S, Hubbard BK, et al. Dissociation of hepatic steatosis and insulin resistance in mice overexpressing DGAT in the liver. Cell Metab 2007;6:69–78. [PubMed: 17618857]

34). Warner GJ, Stoudt G, Bamberger M, Johnson WJ, Rothblat GH. Cell toxicity induced by inhibition of acyl coenzyme A:cholesterol acyltransferase and accumulation of unesterified cholesterol. J Biol Chem 1995;270:5772–5778. [PubMed: 7890706]

35). Yao PM, Tabas I. Free cholesterol loading of macrophages is associated with widespread mitochondrial dysfunction and activation of the mitochondrial apoptosis pathway. J Biol Chem 2001;276:42468–42476. [PubMed: 11533046]

36). Farese RV Jr., Zechner R,Newgard CB, Walther TC. The problem of establishing relationships between hepatic steatosis and hepatic insulin resistance. Cell Metab 2012;15:570–573. [PubMed: 22560209]

37). Jornayvaz FR, Birkenfeld AL, Jurczak MJ, Kanda S, Guigni BA, Jiang DC, et al. Hepatic insulin resistance in mice with hepatic overexpression of diacylglycerol acyltransferase 2. Proc Natl Acad Sci U S A 2011;108:5748–5752. [PubMed: 21436037]

38). Ning T, Zou Y, Yang M, Lu Q, Chen M, Liu W, et al. Genetic interaction of DGAT2 and FAAH in the development of human obesity. Endocrine 2017;56:366–378. [PubMed: 28243972]

39). Liu DJ, Peloso GM, Yu H, Butterworth AS, Wang X, Mahajan A, Saleheen D, Emdin C, et al. Exome-wide association study of plasma lipids in >300,000 individuals. Nat Genet 2017;49:1758–1766. [PubMed: 29083408]

40). The Emerging Risk Factors Collaboration. Major lipids, apolipoproteins, and risk of vascular disease. JAMA 2009;302: 1993–1915. [PubMed: 19903920]

41). Vitali C, Khetarpal SA, Rader DJ. HDL cholesterol metabolism and the risk of CHD: new insights from human genetics. Curr Cardiol Rep 2017;19:310–312.

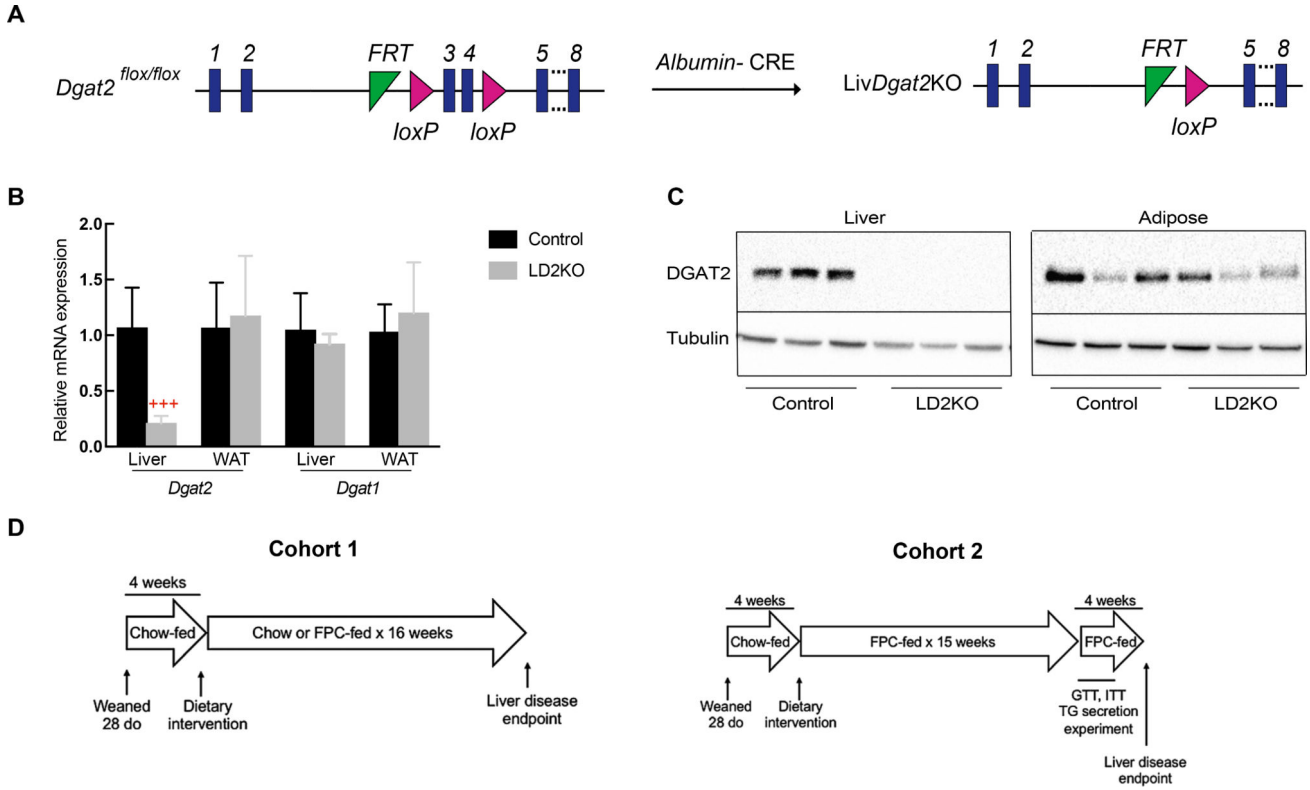

FIG. 1.

Generation of a murine model of DGAT2 deficiency in hepatocytes and experimental design. (A) Map of the *Dgat2* floxed allele. When *Dgat2*$^{flox/flox}$ mice are crossed with mice expressing Cre recombinase under an albumin promotor, exons 3 and 4 of *Dgat2* are deleted. (B) Hepatocyte-specific *Dgat2* knockout (Liv*Dgat2*KO) results in ~80% less *Dgat2* mRNA expression in liver lysates of Liv*Dgat2*KO mice than in controls. *Dgat1* expression is similar in control and Liv*Dgat2*KO livers. n = 4–6/genotype. (C) Western blotting analysis showing no detectable DGAT2 protein in liver lysates from Liv*Dgat2*KO mice. (D) Experimental design for two cohorts of control and Liv*Dgat2*KO mice on chow and FPC diets. $^{+++}P <$ 0.0005. Abbreviations: GTT, glucose tolerance test; ITT, insulin tolerance test; WAT, white adipose tissue.

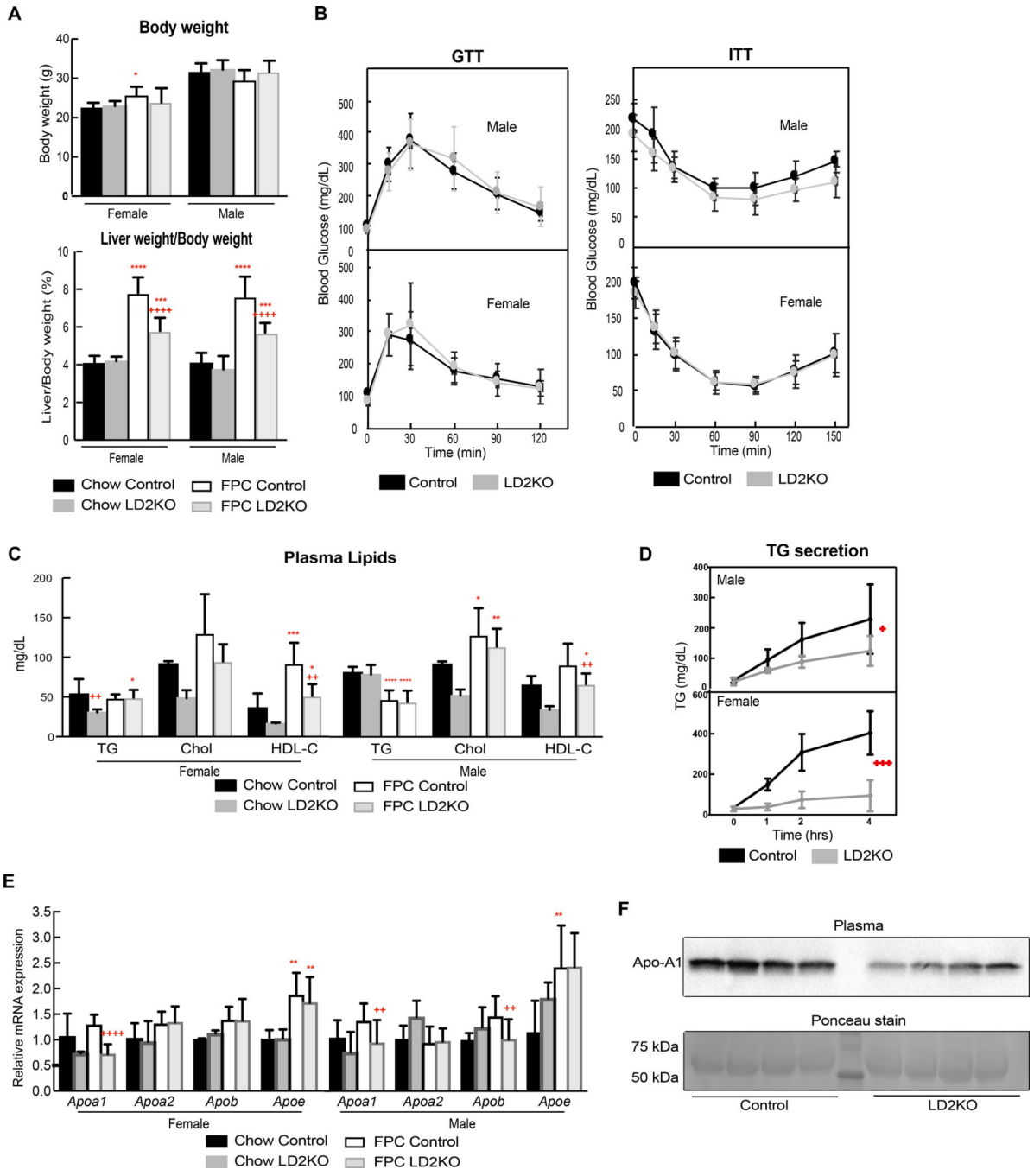

FIG. 2.

Metabolic parameters in control and Liv*Dgat2*KO mice on chow and FPC diets. (A) LivDgat2KO and control mice have similar body weights on chow or FPC diet for 16 weeks. Liver to body weight is lower in Liv*Dgat2*KO animals fed the FPC diet. Age 24 weeks, n = 7–10/genotype on chow diet, n = 10 females/genotype on FPC, 15–18 males/genotype on FPC. (B) Glucose and insulin tolerance tests performed in mice fed an FPC diet for 14–15 weeks. For GTT, mice were fasted overnight, then 2 mg/g of glucose was administered intraperitoneally, and blood glucose measured at times as indicated. For ITT, mice were

fasted for 4 hours, then 1 U/kg of insulin was administered intraperitoneally, and blood glucose measured at times as indicated. n = 9–13 males/genotype, n = 8–15 females/genotype. (C) Plasma TG, cholesterol (Chol), and HDL-C levels in mice fed chow or FPC diets for 16 weeks. n = 5 males/genotype, n = 4–5 females/genotype on chow diet. n = 11–16 males/genotype, n = 7 females/genotype on FPC diet. (D) Plasma TG levels. After a 4-hour fast, mice were administered Tyloxapol at time 0 and subsequent TG levels were measured at indicated time points. n = 6 males/genotype, n = 5 females/genotype. (E) Real-time PCR analysis of apolipoprotein genes in mice on chow and FPC diets. *Apoa1* gene expression is decreased in Liv*Dgat2*KO animals on FPC diet. n = 4–5 females and males/genotype on chow, n = 10 females/genotype, 15–18 males/genotype on FPC. (F) Immunoblotting showing less apo-A1 in plasma of male mice on an FPC diet. Ponceau stain, with albumin band, of the same blotting is also shown. n = 4/genotype. *Indicates statistical difference between diets, $*P < 0.05$; $**P < 0.005$; $***P < 0.0005$; $****P < 0.0001$. $^{+}$Indicates statistical difference between genotypes, $^{+}P < 0.05$; $^{++}P < 0.005$; $^{+++}P < 0.0005$; $^{++++}P < 0.0001$. Abbreviations: GTT, glucose tolerance test; ITT, insulin tolerance test.

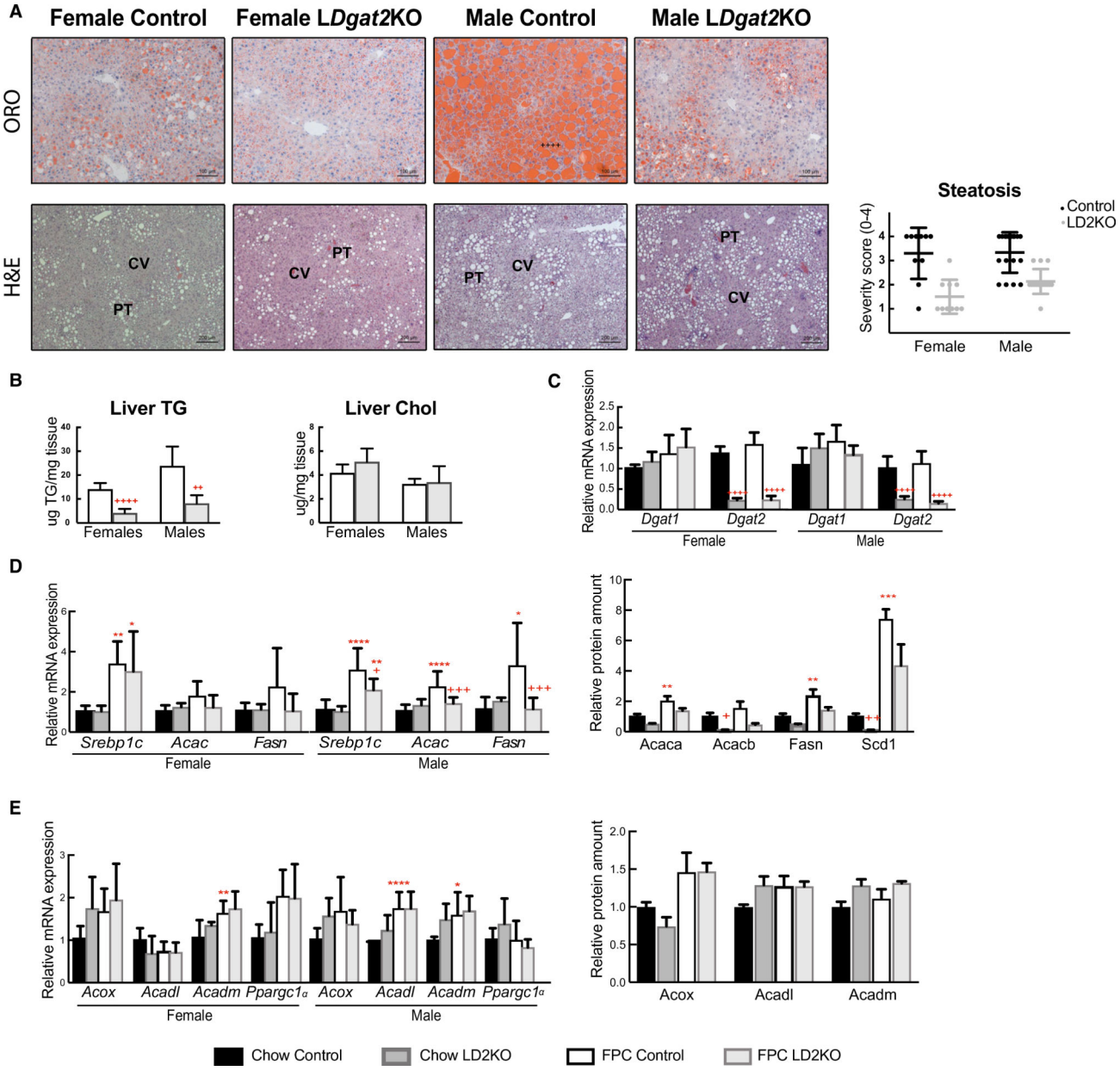

FIG. 3.

Liv*Dgat2*KO mice have improved steatosis on FPC diet. (A) Representative ORO-stained liver sections and steatosis severity scores in mice on FPC diet for 16 weeks. Each symbol represents the score for an individual mouse. n = 10 females/genotype, 15–18 males/genotype. (B) Hepatic TG and total cholesterol content in mice on FPC diet for 16 weeks. n = 8/genotype/sex. (C) Real-time PCR analysis of TG synthesis genes, *Dgat1* and *Dgat2* in this cohort. (D) *De novo* lipogenesis gene expression measured by qPCR and relative protein amounts detected by mass spectrometry in mice on chow and FPC diets. (E) Beta-oxidation gene expression measured by qPCR and relative protein amounts detected by mass spectrometry in mice on chow and FPC diets. n = 4–5 females and males/genotype on chow. n = 10 females/genotype, 15–18 males/genotype on FPC for gene expression data. n = 3

males/genotype/diet for proteomic data. *Indicates statistical difference between diets, *$P <$ 0.05; **$P < 0.005$; ****$P < 0.0001$. $^{+}$Indicates statistical difference between genotypes, $^{+}P <$ 0.05; $^{++}P < 0.005$; $^{+++}P < 0.0005$; $^{++++}P < 0.0001$. Abbreviations: *Acac*, acyl-CoA carboxylase; *Acadl*, acyl-CoA dehydrogenase long chain; *Acadm*, acyl-CoA dehydrogenase medium chain; *Acox*, acyl Co-A oxidase; CV, central vein; Chol, cholesterol; *Fasn*, fatty acid synthase; *Ppargc1α*, peroxisome proliferator-activated receptor γ co-activator 1α; PT, portal triad.

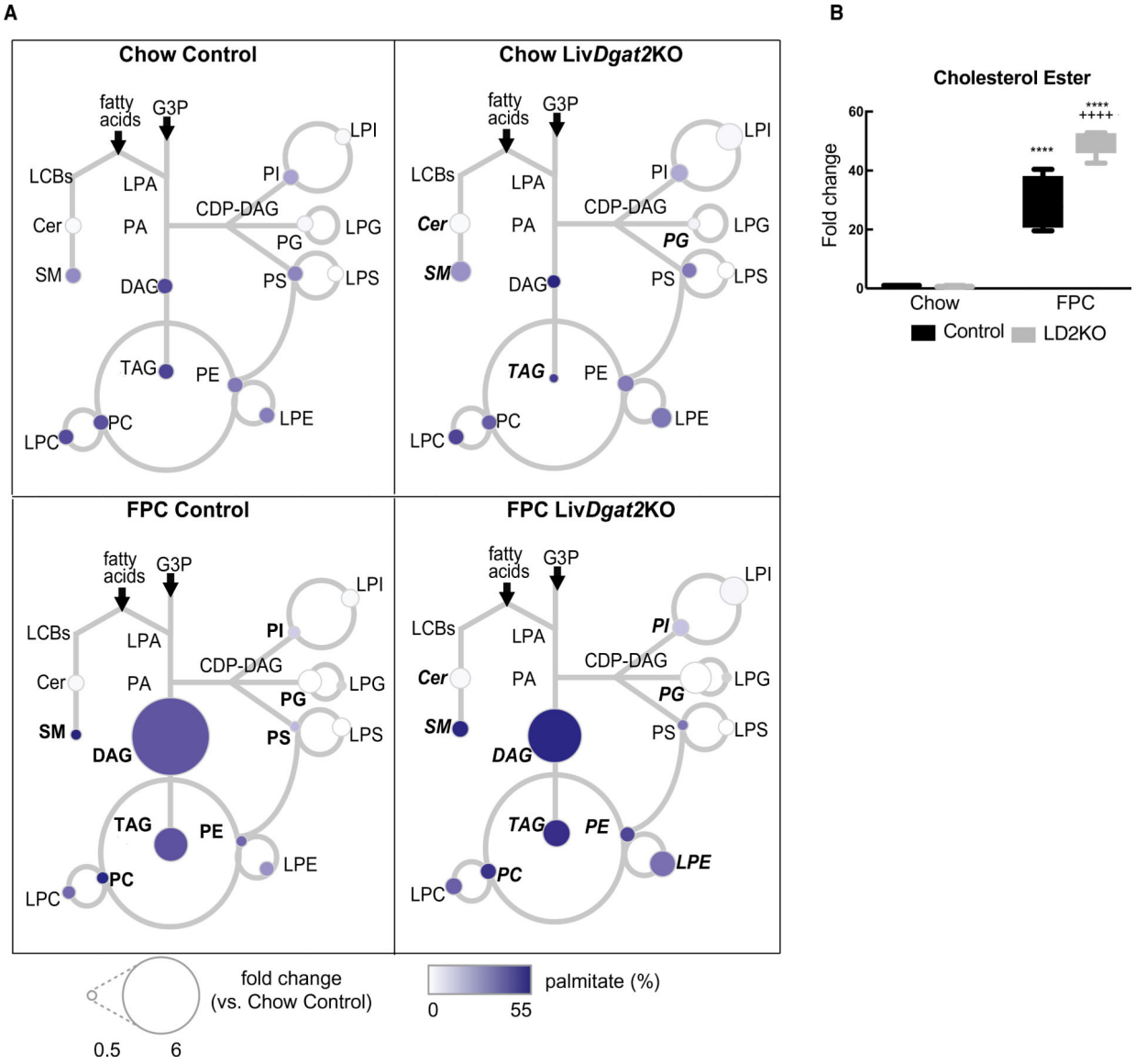

FIG. 4.

Summary of lipid class changes in Liv*Dgat2*KO mice fed an FPC diet. (A) Changes in lipid class abundance and palmitate content of lipids. Data are displayed as fold change compared to chow-fed control mice (Chow Control). Bold in lower left panel indicates significant difference between Chow Control and FPC Control. Bold Italic indicates significant difference between genotypes. (B) Change in cholesterol esters between the groups, compared to chow-fed control mice. N = 4–5 male mice/group. *Indicates statistical difference between diets, ****$P < 0.0001$. $^{+}$Indicates statistical difference between genotypes, $^{++++}P < 0.0001$. Abbreviations: G3P, glycerol 3-phosphate; LCB, long-chain sphingoid bases; Cer, ceramide; SM, sphingomyelin; LPA, lysophosphatidic acid; PA, phosphatidic acid; DAG, diacylglycerol; TAG, triglyceride; PC, phosphatidylcholine; LPC, lysophophatidylcholine; PE, phosphatidylethanolamine; LPE, lysophosphatidylethanolamine; CDP-DAG, cytidine diphosphate diacylglycerol; PI,

phosphatidylinositol; LPI, lysophosphatidylinositol; PG, phosphatidylglycerol; LPG, lysophosphatidylglycerol; PS, phosphatidylserine; LPS, lysophosphatidylserine.

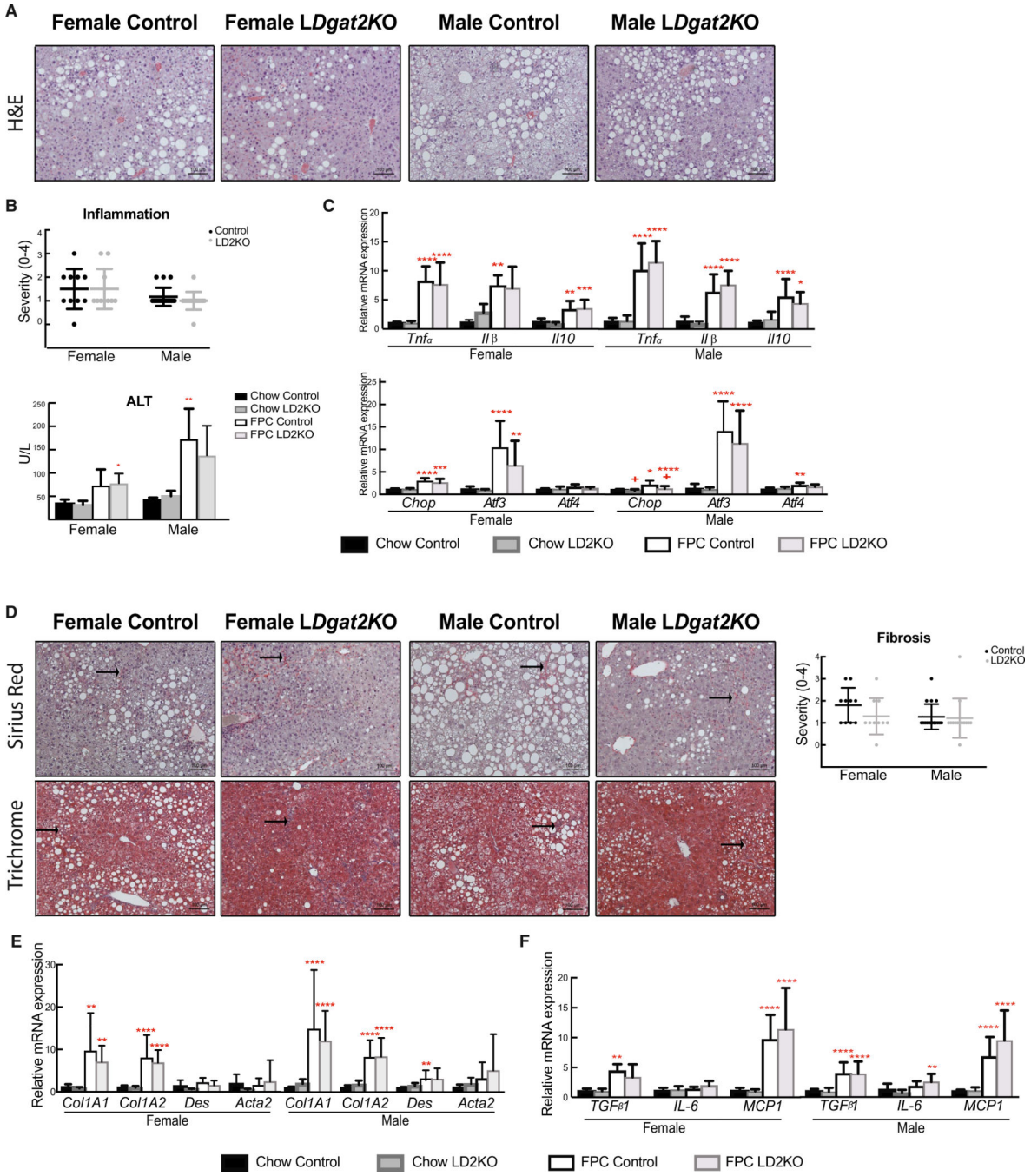

FIG. 5.

Lowering hepatic TG content does not worsen hepatic inflammation or fibrosis in Liv*Dgat2*KO mice fed an FPC diet. (A) H&E-stained liver sections from mice on the FPC diet for 16 weeks. (B) Inflammation severity scores and ALT levels in mice on FPC diet for 16 weeks. Each symbol on inflammation graph represents the score for an individual mouse. n = 10 females/genotype, 15–18 males/genotype for inflammation scores. n = 7–9/gender/genotype for ALT. (C) Real-time PCR analysis of inflammatory response and ER stress genes in mice on chow and FPC diets. (D) Representative Sirius Red–, Masson's trichrome–

stained liver sections for mice on FPC diet for 16 weeks; arrows point to areas of fibrosis. Fibrosis scores are also shown; each symbol represents the score for an individual mouse. n = 10 females/genotype, 15–18 males/genotype. (E) Real-time PCR analysis of fibrosis-associated genes in mice on chow and FPC diets. For gene expression data: n = 4–5 females and males/genotype on chow, n = 10 females/genotype, 15–18 males/genotype on FPC. (F) Real-time PCR analysis of genes associated with induction hepatic stellate cell activation. *Indicates statistical difference between diets, *$P < 0.05$; **$P < 0.005$; ***$P < 0.0005$; ****$P < 0.0001$. $^{+}$Indicates statistical difference between genotypes, $^{+}P < 0.05$. Abbreviations: *Acta2*, smooth muscle actin α; *Atf3*, activating transcription factor 3; *Atf4*, activating transcription factor 4; *Chop*, CCAAT-enhancer-binding protein–homologous protein; *Col1A1*, collagen type 1α1; *Col1A2*, collagen type 1α2; *Des*, desmin; *Ilβ*, interleukin β; *Il10*, interleukin 10; *MCP1*, monocyte chemoattractant protein 1; *TGFβ1*, transforming growth factor beta 1; *Tnfα*, tumor necrosis factor α.